Journal of Cellular Biochemistry 97:984–998 (2006)

Expression Profile of IGF System During Lung Injury and Recovery in Rats Exposed to Hyperoxia: A Possible Role of IGF-1 in Alveolar Epithelial Cell Proliferation and Differentiation

Telugu A. Narasaraju,[1] Haifeng Chen,[1] Tingting Weng,[1] Manoj Bhaskaran,[1] Nili Jin,[1] Jiwang Chen,[1] Zhongming Chen,[1] Mala R. Chinoy,[2] and Lin Liu[1]*

[1]Department of Physiological Sciences, Oklahoma State University, Stillwater, Oklahoma 74078
[2]Department of Surgery, Pennsylvania State University College of Medicine, Hershey Medical Center, Hershey, Pennsylvania 17033

Abstract Although several studies have shown that an induction of insulin-like growth factor (IGF) components occurs during hyperoxia-mediated lung injury, the role of these components in tissue repair is not well known. The present study aimed to elucidate the role of IGF system components in normal tissue remodeling. We used a rat model of lung injury and remodeling by exposing rats to >95% oxygen for 48 h and allowing them to recover in room air for up to 7 days. The mRNA expression of IGF-I, IGF-II, and IGF-1 receptor (IGF-1R) increased during injury. However, the protein levels of these components remained elevated until day 3 of the recovery and were highly abundant in alveolar type II cells. Among IGF binding proteins (IGFBPs), IGFBP-5 mRNA expression increased during injury and at all the recovery time points. IGFBP-2 and -3 mRNA were also elevated during injury phase. In an in vitro model of cell differentiation, the expression of IGF-I and IGF-II increased during trans-differentiation of alveolar epithelial type II cells into type-I like cells. The addition of anti-IGF-1R and anti-IGF-I antibodies inhibited the cell proliferation and trans-differentiation to some extent, as evident by cell morphology and the expression of type I and type II cell markers. These findings demonstrate that the IGF signaling pathway plays a critical role in proliferation and differentiation of alveolar epithelium during tissue remodeling. J. Cell. Biochem. 97: 984–998, 2006.

Key words: IGF; lung injury; tissue repair; trans-differentiation; alveolar type II cells

In the treatment of premature babies and patients suffering from respiratory distress syndrome supplemental oxygen (hyperoxia) is inevitably used to maintain adequate blood oxygen. A short-term exposure to hyperoxia causes endothelial and epithelial injury, while a prolonged exposure leads to interstitial edema, mesenchymal cell proliferation, and fibrin deposition [Yam et al., 1978; Crapo et al., 1980; Barazzone et al., 1996; Narasaraju et al., 2003]. Tissue repair occurs when these injured animals are allowed to recover in normal air. Pulse-chase labeling studies in mice after hyperoxia exposure have shown that type II cells proliferate and differentiate into type I cells between day 2 and 4 of recovery [Adamson and Bowden, 1974b; Harris et al., 1991]. Proliferation of fibroblasts also occurs during tissue remodeling. The regulation of fibroblast proliferation during tissue remodeling is critical in order to achieve normal repair. The increase in fibroblasts or matrix deposition causes an abnormal repair, leading to the tissue fibrosis observed in bronchopulmonary dysplasia, a disease associated

Abbreviations used: IGF-I and -II, insulin-like growth factor-I and -II; IGF-1R and -2R, IGF-I and -II receptor; IGFBP 1–6, IGF binding protein 1–6; DAPI, 4,6-diamidino-2-phenyindole; MPA, *Maclura promifera*; PBS, phosphate-buffered saline; FBS, fetal bovine serum; TBS-T, Tris-buffered saline containing 0.1% Tween-20.

Grant sponsor: NIH; Grant numbers: R01 HL-52146, R01 HL-071628; Grant sponsor: OCAST; Grant number: HR01-093; Grant sponsor: AHA heartland affiliate (to LL); Grant number: 0255992Z.

*Correspondence to: Lin Liu, PhD, Department of Physiological Sciences, Oklahoma State University, 264 McElroy Hall, Stillwater, Oklahoma 74078.
E-mail: liulin@okstate.edu

Received 9 August 2005; Accepted 10 August 2005
DOI 10.1002/jcb.20653

with ventilation therapy [O'Brodovich and Mellins, 1985; Adamson et al., 1988; Bhatt et al., 2001]. The factors influencing tissue remodeling may include hormones, growth factors, pro/anti-inflammatory cytokines, proteases, and other signaling molecules [Harris et al., 1991; Nici et al., 1996].

Insulin-like growth factors (IGFs) have been reported to play an important role in cell proliferation and differentiation in a variety of cells [Cohick and Clemmons, 1993; Jones and Clemmons, 1995; Stewart and Rotwein, 1996]. IGFs mediate their actions through a cell surface receptor, IGF-1 receptor (IGF-1R). Stimulation of IGF-1R causes activation of various intracellular signaling pathways, which ultimately promote the cell cycle progression. The bioavailability of IGFs is regulated by six structurally related IGF binding proteins 1–6 (IGFBPs 1–6) [Han et al., 1988; Delhanty et al., 1993; Jones et al., 1993]. IGF system components are critical in normal lung growth and development [Wallen and Han, 1994; Maitre et al., 1995]. A high expression of IGFs in rat lungs during days 5–14 of the postnatal period was observed. The IGF system components may also actively participate in lung repair after injury. IGF-I and IGF-II are expressed in different cell types in the lung, including fibroblasts, epithelial cells, and macrophages. Several studies have demonstrated the role of IGF system components in cell proliferation during hyperoxia-mediated lung injury [Cazals et al., 1999; Chetty and Nielsen, 2002]. In rats exposed to 85% oxygen for 6 and 14 days, increased expression of IGF-I was found, which showed proliferative effects on alveolar type II and fibroblast cells in the lungs [Han et al., 1996]. IGF-II expression was also found in alveolar type II cells after exposure to hyperoxia [Veness-Meehan et al., 1997]. The increase in IGF-I was found to be associated with an increase in fibroblast proliferation and migration towards human tracheal broncho-epithelial when co-cultured in vitro [Chetty et al., 1999], indicating that IGFs cause proliferation of different cell types by acting in a paracrine or autocrine manner. Inhibition of type II cell proliferation was associated with accumulation of the IGF binding protein, IGFBP-2, suggesting the regulation of IGF's action by IGFBP-2 [Cazals et al., 1999].

Although several studies demonstrated the involvement of IGF system components in hyperoxia-mediated injury, most of these studies were confined to the lung injury models, and the status of these components during the tissue repair is not well studied. The present study aimed to examine the expression profile of the IGF system components during lung injury and recovery. A rat model of lung injury and normal remodeling was used by exposing animals to hyperoxia and allowing them to recover in room air. Histopathological and immunohistochemical analyses were carried out to evaluate lung injury. Quantitative real-time PCR and immunohistochemistry were performed to determine the expression profiles of IGF system components during the lung injury and repair. Furthermore, an in vitro model of alveolar epithelial cell differentiation was used to substantiate the in vivo results to probe for the role of these IGF system components in epithelial cell proliferation and differentiation.

MATERIALS AND METHODS

Materials

Rat IgG, 4,6-diamidino-2-phenylindole (DAPI), phenylmethylsulfonyl fluoride (PMSF), deoxyribonuclease-1, and *n*-propyl gallate were purchased from Sigma (St. Louis, MO). Elastase was from Worthington Biochemical Corporation (Lakewood, NJ). Rabbit anti-IGF-1Rβ and goat anti-purinergic receptor P2X7 antibodies were from Santa Cruz Biotechnology (Santa Cruz, CA). Anti-rat CD45 antibodies were from BD Bioscience (San Jose, CA). Monoclonal anti-LB-180 antibodies were from Covance (Richmond, CA). Monoclonal anti-T1 α antibodies were kindly provided by Dr. Mary C. Williams (Boston University) and Dr. Antoinette Wetterwald (University of Berne, Switzerland). Mouse anti-IGF-I and anti-IGF-II antibodies were obtained from Upstate Biotechnology (Lake Placid, NY). Mouse anti-glyceraldehyde-3-phosphate dehydrogenase (GAPDH) antibodies were from Ambion (Austin, TX). Mouse anti-Syrian hamster T1 α antibodies were obtained from Developmental Studies Hybridoma Bank (University of Iowa). *Maclura promifera* (MPA)-FITC was from EY laboratories (San Mateo, CA). Rabbit Cy3-conjugated anti-mouse antibodies were from Jackson Immuno Research laboratories (West Grove, PA). Alexa 546-conjugated anti-rabbit or anti-goat antibodies were from Molecular Probes (Eugene, OR). Anti-rat

IgG and anti-mouse IgG dynabeads were from Dynal Biotech (Lake Success, NY). Dc Protein assay kit, horseradish peroxidase-conjugated anti-mouse and anti-rabbit antibodies were from Bio-Rad (Hercules, CA). Enhanced chemiluminescence detection system was from Amersham Biotech (Piscataway, NJ). TRI Reagents were from Molecular Research Center, Inc. (Cincinnati, OH). M-MLV reverse transcriptase were from Invitrogen (Carlsbad, CA). GeneClean Turbo for PCR kit from (Q-Bio gene, CA). DMEM/F12 medium was from American Type Culture Collection (Rockville, CA). Quantitect SYBR Green PCR kit was from Qiagen (Valencia, CA). Penicillin, streptomycin, and fetal bovine serum (FBS) were from GIBCO (Grand Island, NY).

Hyperoxia Model of Lung Injury and Repair

Pathogen-free male Sprague–Dawley rats (250–275 g) were placed in a sealed Plexiglas chamber ($90 \times 45 \times 45$ cm) and exposed to >95% medical grade oxygen for 48 or 60 h. The flow rate was maintained at 8 L/min using a flow meter (Vacu-Med, Ventura, CA). The oxygen concentration was continuously monitored with an oxygen analyzer (Vacu-med, Ventura, CA). Soda lime was placed in the chamber to remove CO_2. Animals had free access to food and water. At the end of hyperoxia exposure animals were allowed to recover in normal air and sacrificed at different time intervals (0, 1, 3, 5, and 7 days). The control rats were housed in room air. Animals were anesthetized with intraperitoneal injections of ketamine (40 mg/kg) and xylazine (8 mg/kg). A tracheotomy was performed. Rat lungs were ventilated with a rodent ventilator and perfused with phosphate-buffered saline (PBS). Lungs were lavaged with 7 ml of normal saline four times. Tissue samples were immediately frozen in liquid nitrogen and stored at −80°C. For histopathological analysis the trachea was cannulated and the lungs were fixed by instilling 4% formaldehyde in PBS into the trachea under a hydrostatic pressure of 20 cm. After 24 h incubation the lungs were washed in PBS, dehydrated in graded alcohol and xylene, and embedded in paraffin (60°C). Paraffin-embedded lungs were sectioned (4 μm) and placed on polysine glass slides. The slides were deparaffinized with xylene, rehydrated with graded alcohol and PBS, and stained with hematoxyline and eosin.

Immunohistochemistry

Lung sections were permeabilized with 0.3% Triton X-100 in PBS for 20 min, blocked with 10% FBS in PBS for 20 min, and incubated overnight at 4°C with primary antibodies: mouse anti-T1 α (1:100), anti-IGF-I (1:200), IGF-II (1:500), or anti-IGF-1Rβ (1:200). Antigen retrieval was carried out for IGF-I, IGF-II, and IGF-1Rβ by boiling the sections in a microwave for 5 min in 20 mM citrate buffer (pH 6.0) before permeabilization. After being washed three times in PBS for 5 min the slides were incubated with Cy3-conjugated anti-mouse or Alexa 546-conjugated anti-rabbit Ig G (1:500) for 1 h at 4°C. The slides were washed once with PBS and then stained with MPA-FITC (1:250) for 10 min. The slides used for triple staining were further stained with DAPI (1 μg/ml) for 5 min. Finally, the slides were mounted with anti-fade medium (5% *n*-propyl gallate and 80% glycerol in PBS) and examined using a Nikon Eclipse E600 fluorescence microscope.

Alveolar Type I and Type II Cell Counting

Triple labeled lung tissue sections using T1 α (type I cells), MPA (type II cells), and DAPI (nuclei) were counted for alveolar type I and type II cells. Type II cells can be easily identified by FITC-labeled MPA, which showed a typical corner staining. During cell counting, we avoided the red blood cells, which give auto fluorescence, but do not show DAPI staining. Type 1 cells, when labeled with T1 α antibodies exhibited a continuous staining. However, with the aid of DAPI staining and careful elimination of type II cells, endothelial cells, and fibroblasts, we were able to estimate type I cells. The type I cells showing discontinuous staining due to injury were not counted. A total of 300 alveoli were counted per slide. Furthermore, total air space perimeters, covered by alveolar type II and type I cells was determined by measuring the length of MPA (green) and T1 α (red) staining using Image-Pro Plus software as described [Kitterman et al., 2002]. About 30 fields were analyzed per slide, and the ratios of type I to type II length was determined.

RNA Extraction and cDNA Synthesis

Total RNA from lung samples and in vitro cultured cells was prepared using Tri Reagents. After being washed in 70% ethanol, RNA was solubilized in water and treated with DNase I to

remove contaminating genomic DNA. One microgram of total RNA from the samples was reverse transcribed into cDNA with 200 U M-MLV reverse transcriptase and random primers.

Real-Time PCR Using SYBR Green I

Gene sequence information was obtained using nucleotide databases (www.ncbi.nlm.nih.gov/Entrez), and all primer sequences were assessed for specificity with non-redundant basic local alignment search using Primer Express Software version 1.0 (PE Applied Biosystems, Foster City, CA). The primer sequences for IGF system components are given in Table I. Traditional PCR was performed to obtain standards for quantitatively assessing mRNA copy number and relative abundance of IGF system components. The PCR product was purified by GeneClean Turbo for PCR kit, quantified and serially aliquoted into successive, 10-fold diminishing dilutions (from 1×10^8 to 1×10^1 copies/5 μl) in sterile water. Copy number determination was made using the following formula: copies/ml = $(6.023 \times 10^{23} \times 5 \times 10^{-5} \times OD_{260} \times$ dilution factor)/molecular weight. Real-time PCR was performed using an ABI PRISM 7700 system (PE Applied Biosystems). The amplifications were carried out in a 96-well plate in a 25 μl reaction volume containing 12.5 μl SYBR master mix, 0.3 μM of each forward and reverse primer pair, 1 μl of cDNA, 1 μl of Mg^{2+}, and 9 μl of H_2O. Each sample was prepared in duplicate and the experiment was repeated five times. The thermal cycling conditions used were: 95°C for 15 min, followed by 40 cycles of 95°C for 15 s, 60°C for 30 s, and 72°C for 30 s. The fluorescence acquisition for IGF-I and insulin receptor substrate-1 (IRS-1) was made at 74°C for 30 s, T1 α at 76°C for 30 s, and all other genes at 78°C for 15 s. The standard curve was generated by plotting log copy numbers of PCR product versus Ct. Copy numbers of the gene in samples were determined from the standard curve. The data were analyzed with the absolute standard curve method using the Sequence Detector 1.9.1, provided by ABI 7700 system. The copy number was normalized with 18S rRNA.

Western Blot Analysis

Frozen lung tissue was homogenized in lysis buffer (10 mM Tris-HCl, pH 7.5, 1% Triton X-100, 1 mM EDTA and 1 mM PMSF, 10 μg/ml aprotonin, and 10 μg/ml leupeptin). Protein concentration was determined by using Dc protein assay kit. Twenty to 40 μg of proteins were separated on 12% polyacylamide gel and transferred onto a nitrocellulose membrane at 100 mAmp for 2 h. The membrane was stained with Ponceau S to check the efficiency of the transfer of proteins, and blocked overnight with 5% dry milk in 100 mM Tris-buffered saline containing 0.1% Tween-20 (TBS-T). The membrane was then washed twice in TBS-T (5 min each) and incubated with anti-IGF-1Rβ (1:1,000), anti-T1 α (1:500), or anti-GAPDH (1:5,000) antibodies for 3 h at room temperature. The membrane was washed three times (5 min each) in TBS-T, and then incubated with horseradish peroxidase-conjugated anti-rabbit or anti-mouse IgG (1:5,000) for 1 h. The blots were washed three times (5 min each) and the antigens identified using enhanced chemiluminescence detection system and exposure to X-ray film.

Isolation and Culture of Type II Cells From Hyperoxia-Exposed Lungs

Alveolar type II cells from 48 h hyperoxia-exposed lungs were isolated as previously described [Chen et al., 2004a]. In brief, lungs were lavaged and digested with elastase, followed by differential adherence on IgG plates. The unattached cells from IgG plate were further incubated with anti-CD45 (20 μg/ml) and rat IgG (75 μg/ml) for 30 min at 4°C, followed by incubation for 20 min with anti-rat and anti-mouse IgG-conjugated magnetic beads. The cells attached to the magnetic beads were removed by applying them to a magnetic field. The unattached cells were then washed two times with large volumes of RPMI 1640 medium containing 0.5% FBS. Then, the cells were incubated with mouse anti-hamster T1 α antibodies for 30 min at 4°C, followed by the addition of anti-mouse IgG magnetic beads and incubation for 20 min. The unattached cells were separated and stained with harris hematoxylin for purities and yields. The purity of the type II cells was above 92% and the yield was about 20×10^6 cells from one rat. The cells were then seeded onto plastic dishes at a density of 4×10^6 cells/60 mm in DMEM/F12 supplemented with 0.5% FBS and cultured for 1–5 days in the presence or absence of anti-IGF-1Rβ, IGF-I, or IGF-II antibodies (10 μg/5 ml). At each time point TRI reagent was added to the cells and RNA was isolated. For Western blot studies, cells were lysed in lysis buffer. For immocyto-

TABLE I. Primer Sequences for Real Time PCR

Accession number	Gene name	Primer	Sequence
AA924219	*IGF-I*	Forward	CTCCTAAAGACAATGTCGGATAGTT
		Reverse	AACACCTGCCAAATATCAATAATGAG
NM031511	*IGF-II*	Forward	AGTTCTCCCCATCATAGGTCACC
		Reverse	CCGAAGACAGTAGGGAAGAGACAA
J04486	*IGFBP-2*	Forward	ATGTGGACGGAACCATGAACA
		Reverse	GTTGACCTTCTCCCGGAACAC
NM012588	*IGFBP-3*	Forward	TCATCTGAAGTTCCTCAATGTGCT
		Reverse	CTTTGGAAGGGCGACACTGT
M62781	*IGFBP-5*	Forward	AGGAAACTGAGGACCTCGGAAT
		Reverse	CTGTCCGTTCAACTTGCTTCAA
NM_052807	*IGF-1R*	Forward	TCCTGTATCTCAGTGGATCTTCAGA
		Reverse	GCTTGCATATTGAAAAAAGGAAGG
X58375	*IGF-2R*	Forward	CAATGAAAAGCACACACCGAGAT
		Reverse	CTTCCGGGCAAGCATAACTG
NM_012969	*IRS-1*	Forward	AACAAAGAGAGGAAGCCACAGACTT
		Reverse	CCACATTCTTCATTTCCAAAGAGAGA
NM_019358	*T1 α*	Forward	GCCATCGGTGCGCTAGAAGATGATCTT
		Reverse	GTGATCGTGGTCGGAGGTTCCTGAGGT
X01117	*18S rRNA*	Forward	TCCCAGTAAGTGCGGGTCATA
		Reverse	CGAGGGCCTCACTAAACCATC

chemistry, the cells were fixed with 4% paraformaldehyde.

Cell Proliferation Assay

For cell proliferation assay, type II cells were seeded in a 96-well plate. A standard was prepared with increasing cell number (2,000–20,000). Cell proliferation assay was carried out according to the method of Kueng et al. [1989]. Briefly, 3×10^4 cells were seeded in each well. After 48 h culture, cells were washed in PBS and incubated for 10 min in 100 μl of 0.1% (w/v) crystal violet in 50 mM phosphate buffer (pH 7.4) and 1% formaldehyde. Plates were washed three times to remove unbound dye. The dye, taken up by the cells, was distained 30 min with 100 μl per well of 33% (v/v) acetic acid with shaking. Plates were then read at 570 nm. Data were expressed as a percentage of change in absorbance of the control cells.

Statistical Analysis

Data are expressed as mean ± SE. Statistical analyses were performed by ANOVA, followed by Dunn's or Student's *t*-test using the software Sigma Stat 2.03. Significance was assigned at $P < 0.05$.

RESULTS

Hyperoxia Model of Lung Injury and Repair

Our previous studies have shown that the exposure of rats to hyperoxia for 48, 60, and 72 h resulted in mild, moderate, and severe injuries, respectively [Narasaraju et al., 2003]. In the present study the animals exposed for 48 and 60 h were compared for histopathology during injury and recovery. Histological analysis revealed alveolar type II cell hyperplasia in 48 h-exposed and day 1–3 recovering rats (Fig. 1). Alveolar epithelium was disrupted after 48 h hyperoxia exposure and regained its normal structure during the recovery. At day 1 and 3, the lung showed structural damage, thick mesenchyme, fewer/smaller abnormal airspaces, and almost no secondary septation. The lung in day 7 exhibited significant recovery of the lung with thinner mesenchyme, larger alveolar spaces, and secondary septation. However, the animals exposed for 60 h showed type II cell hyperplasia, epithelial damage, interstitial edema, fibroblast proliferation, and hemorrhage. The thickening of alveolar septa and increased fibroblast proliferation was found until day 7 of the recovery. Perivascular and peribronchieal expansions and high infiltration were observed during injury and all recovery time points for 60 h hyperoxia-exposed lungs (data not shown).

A triple labeling was developed to evaluate the cytological changes in the alveolar epithelium during injury and repair. Alveolar epithelial type I and type II cells were identified by staining with the type I and type II cell-specific markers: T1 α and MPA-FITC, and nuclei with DAPI (Fig. 2A). There was a gradual increase of type II cells during 48 h hyperoxia injury and subsequent recovery (Fig. 2B). The increase in type II cell number was maximum on day 3 of the recovery, decreased dramatically on day 5, and remained the same on day 7. Type I cells decreased significantly during the injury, but increased during the initial recovery up to day 3.

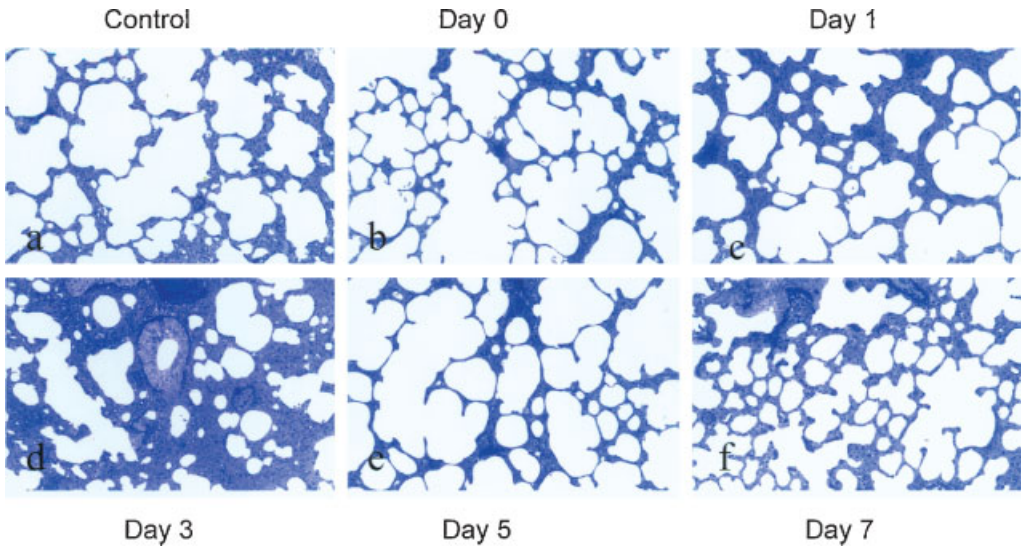

Fig. 1. Histology of hyperoxic lungs. Rats were exposed to >95% of O_2 for 48 h (day 0) and allowed to recover for days 1–7. **a**: The control rats were air-exposed animals. The lungs were aerated and showed alveolar formation and secondary septa development. **b**: The lungs exposed to >95% of O_2 for 48 h showed more expansion of alveolar regions and development of secondary septa. **c**: At day 1, after 48 h exposure of lungs to >95% of O_2, there was significant lung injury seen by thickening of inter-alveolar septa, narrowing of airspaces, and loss of characteristic alveolar structures. **d**: At day 3, after 48 h exposure of lungs to >95% of O_2, pronounced lung injury was observed. The loss of lung structure was visible by highly thickened inter-alveolar areas with almost complete loss of characteristic alveolar structures. **e**: At day 5, after 48 h exposure of lungs to >95% of O_2, repair process must be in place, as reformation of alveolar structures was observed. Some inter-alveolar thickenings persisted. **f**: At day 7, after 48 h exposure of lungs to >95% of O_2, several new alveolar structures were formed and despite some persistent thickenings of inter-alveolar structures, the lungs looked relatively normal due to significant repair processes that may have occurred in 7 days after exposure. All magnifications: ×200. [Color figure can be viewed in the online issue, which is available at www.interscience.wiley.com.]

It remained the same with no significant changes in cell number between day 5 and day 7 of the recovery. We also measured ratios of total lengths of type I and type II cells covered by T1 α and MPA [Kitterman et al., 2002]. The changes in the ratio were consistent with the type I cell counts (Fig. 2B). In contrast, in the 60 h hyperoxia-exposed group, the type II cell number dropped on day 1, increased to maximum on day 3, and decreased by day 5 (data not shown). Type I cell number decreased until day 3 and increased on day 5 of the recovery. These results indicate that hyperoxia exposure for 48 h causes mild injury in lung and mostly damaged cells were alveolar type I epithelial cells. As the recovery for 7 days lead to normal alveolization in the 48 h-exposed group, we selected a 48 h exposure time for the subsequent experiments.

mRNA Expression of IGF System Components During Injury and Tissue Remodeling

The mRNA levels of IGF system components (IGF-I, II, IGF-1R, 2R, IGFBP-2, 3, 5, and IRS-1) were determined by quantitative real time PCR using SYBR Green detection system. The data were normalized using 18S rRNA. As shown in Figure 3A, IGF-II and IRS-1 were expressed lower in the lung than other components of the IGF system. IGF-I and IGF-II mRNA levels increased 1.5- and 2.6-fold on day 0, respectively, and decreased to the control level on day 1–7 of the recovery (Fig. 3B). The levels of IGF-1R increased 3.6-fold on day 0, and reduced to the control level on day 1 (Fig. 3C). However, its expression showed a slight increase on day 7. IGF-2R showed no changes except a 2.2-fold increase on day 0. Among IGFBPs, IGFBP-5 showed an increase during the injury and at day 1–3 of the recovery, and gradually decreased at day 5–7 (Fig. 3D). IGFBP-2 showed an 4.6-fold increase at day 0 and decreased to the normal level by day 1. IGFBP-3 increased twofold at day 0 and then dropped below the control level during the recovery. IRS-1 expression increased 2.3-fold on day 0 and reduced to the normal level during the recovery time intervals (Fig. 3E).

Localization of IGF-I, IGF-II, and IGF-1R in the Lung

Immunostaining for IGF-I and IGF-II in the air-exposed lungs was most abundant in alveo-

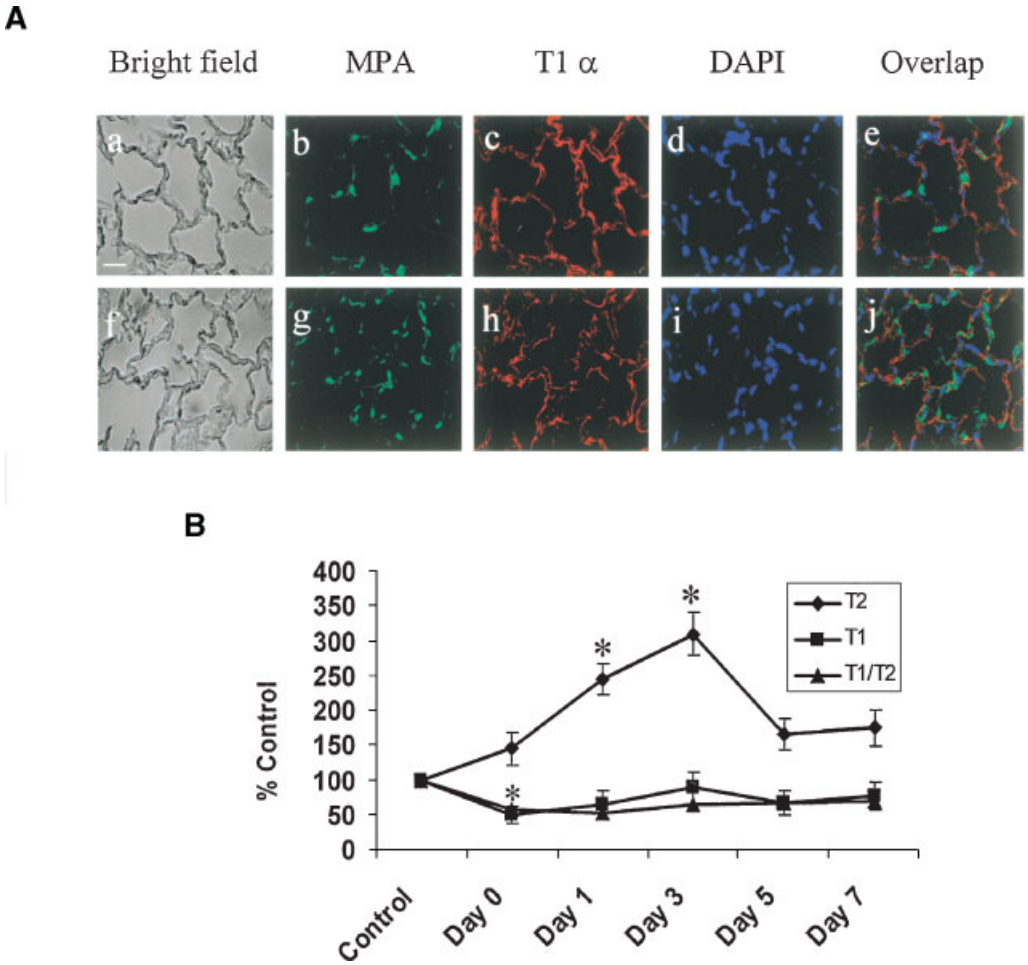

Fig. 2. Effect of hyperoxia on alveolar epithelial cells. Deparaffinized lung sections from air-exposed (control) and 48 h hyperoxia-exposed (day 0) and recovering (day 1, 3, 5, and 7) rats were triple-labeled for type I cells, type II cells, and nuclei using specific markers. Type II cells were stained with MPA-FITC (green). Type I cells were identified by T1 α antibodies and Cy3-conjugated anti-mouse IgG (red). DAPI staining was used to visualize nuclei (blue). **Panel A** shows representatives of bright field and immunofluorescence images of control lungs (**a**–**e**) and 48 h hyperoxia-exposed lungs (**f**–**j**). a, f: bright field; b, g: MPA staining of type II cells; c, h: T1 α staining of type I cells; d, i: DAPI staining of nuclei; and e, j: overlap images. Scale bar, 20 μm. **Panel B** shows the changes in the numbers of alveolar epithelial type I and type II cells. Alveolar type I (T1) and type II (T2) cells were counted based on triple labeling. At least 300 alveoli were counted. The ratios of lengths covered by type I and type II cell specific marker staining (T1/T2) were measured using integrated morphometry analysis. Data are expressed as a percentage of control. $^*P < 0.05$ versus control, $n = 6$ (six slides from four independent animal groups).

lar epithelium, and also observed in airway epithelium (Fig. 4A,C). Double labeling with MPA-FITC showed that type II cells were the major cells to express IGF-I and IGF-II in alveoli (Fig. 4B,D). Hyperoxia exposure increased IGF-I and II protein expression, and the elevated expression was maintained during the recovery phase until day 5. The controls that primary antibodies were omitted did not show significant signals (data not shown). It is noteworthy that the immunohistochemical analyses of IGF-I and -II protein expressions only provide some qualitative indication. Our attempts on quantitative measurements using Western blots for IGF-I and IGF-II were not successful because of the unsuitable antibodies.

Immunoreactivity for IGF-1R was also most abundant in alveolar epithelial cells and airway epithelium (Fig. 5A). The co-localization of IGF-1R with the type II cell marker, MPA-FITC was also observed (Fig. 5B). The staining increased significantly during the injury and up to day 3 of the recovery. These results were in concurrence with Western blot for IGF-1R, which increased on day 0, 1, and 3 and dropped to the normal level by day 5 of the recovery (Fig. 5C,D).

In vitro Model of Alveolar Epithelial Cell Differentiation

It is well known that alveolar epithelial type II cells trans-differentiate into type I-like cells when cultured on plastic plates. To determine whether IGFs participate in the trans-differentiation, we used the antibodies against IGFs and their receptors to block IGF signaling and examined the consequences of such treatment. Alveolar type II cells were isolated from hyperoxia-exposed lungs with a purity of >92% using our recently modified method [Chen et al., 2004a]. The cells were cultured on plastic dishes

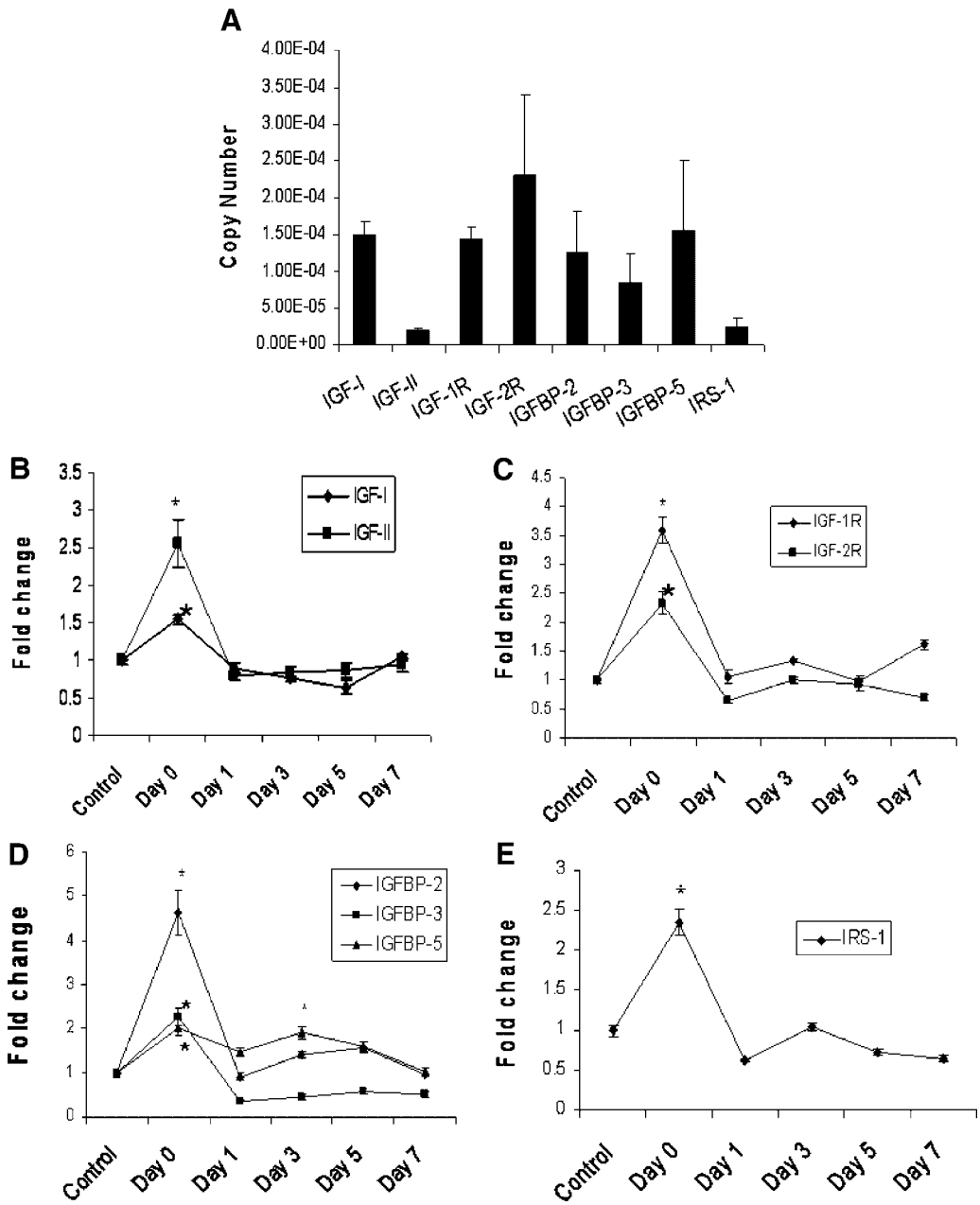

Fig. 3. mRNA expression of IGF system components in injured and repairing lungs. Rats were exposed to >95% O_2 for 48 h (day 0) and allowed to recover for 1-7 days (day 1, 3, 5, and 7). The control was air-exposed rat. Total RNAs were extracted from the lung tissues and the mRNA levels were determined by real time PCR. Data were normalized with 18S rRNA. **A**: Relative abundance of IGF system components in control lungs. The results were expressed as copy number per copy of 18S rRNA. **B–E**: Fold changes of IGF system during injured and repairing lungs. Values are expressed as fold change compared to the control after normalization with 18S rRNA. B: IGF-I and II; (C) IGF-1R and 2R; (D) IGFBP-2, 3, and 5; (E) IRS-1. $^*P < 0.05$ versus control. n = 10 (five animal groups and each assay performed in duplicate).

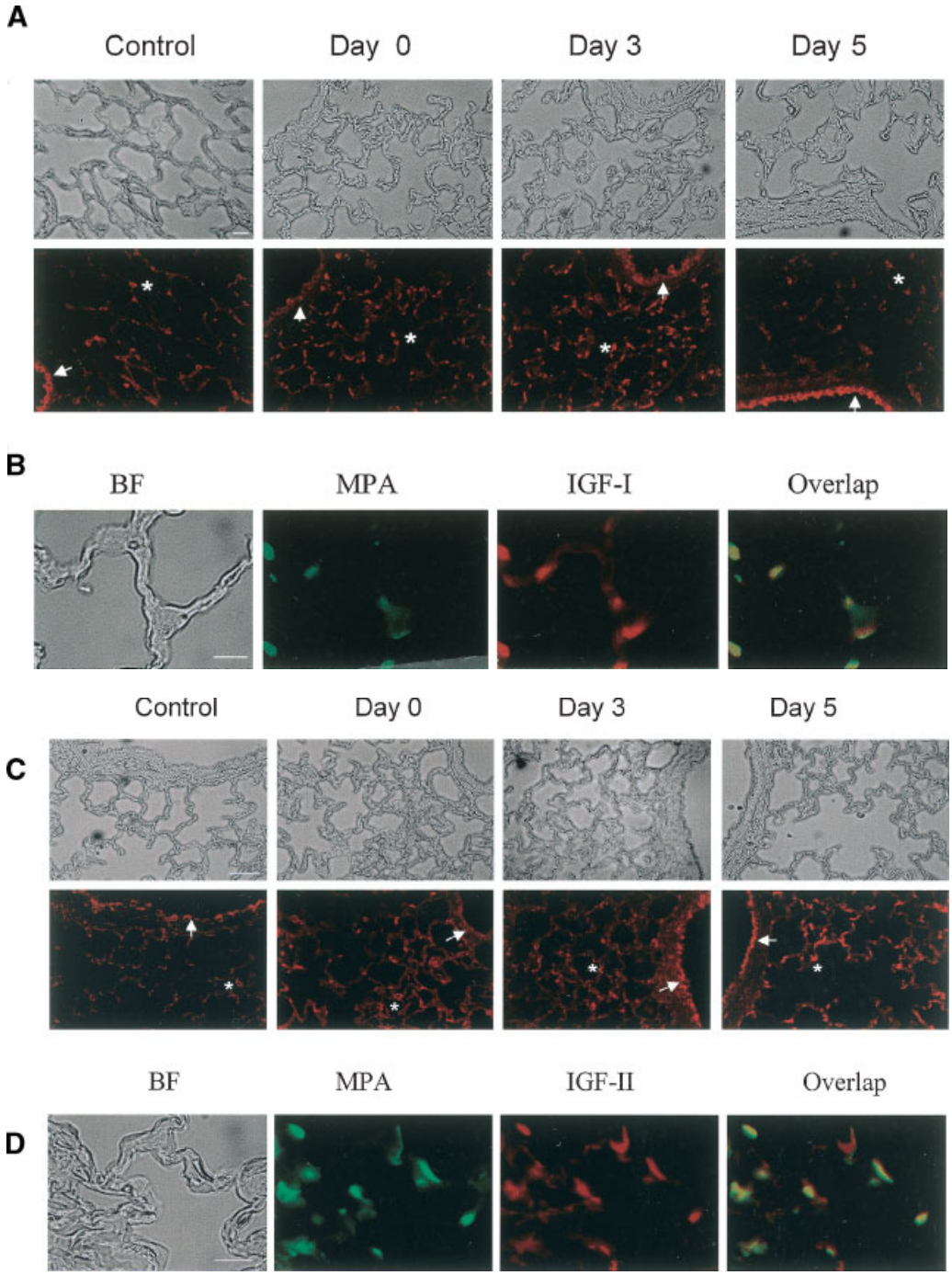

Fig. 4. Immunohistochemistry for IGF-I and IGF-II. **A**, **C**: Deparaffinized lung sections from air-exposed rats (control), 48 h hyperoxia-exposed rats (day 0), and rats recovering for 3 and 5 day rats after the same exposure (day 3 and 5) were stained with anti-IGF-I (A) and anti-IGF-II (C) antibodies. **Upper panels** show bright fields and **lower panels** are immunofluorescence images. Asterisks illustrate the staining in alveolar type II cells and arrows the staining in airway epithelium. **B**, **D**: Double-labeling of normal rat lung tissues using IGF-I (B) or IGF–II (D) antibodies with the type II cell marker, FITC-MPA. The co-localization of IGF-I or IGF-II with MPA in type II cells were noted. BF, bright field; overlap, overlap images from IGF-I or IGF-II and MPA. A representative of three experiments was shown. Scale bar, 20 μm.

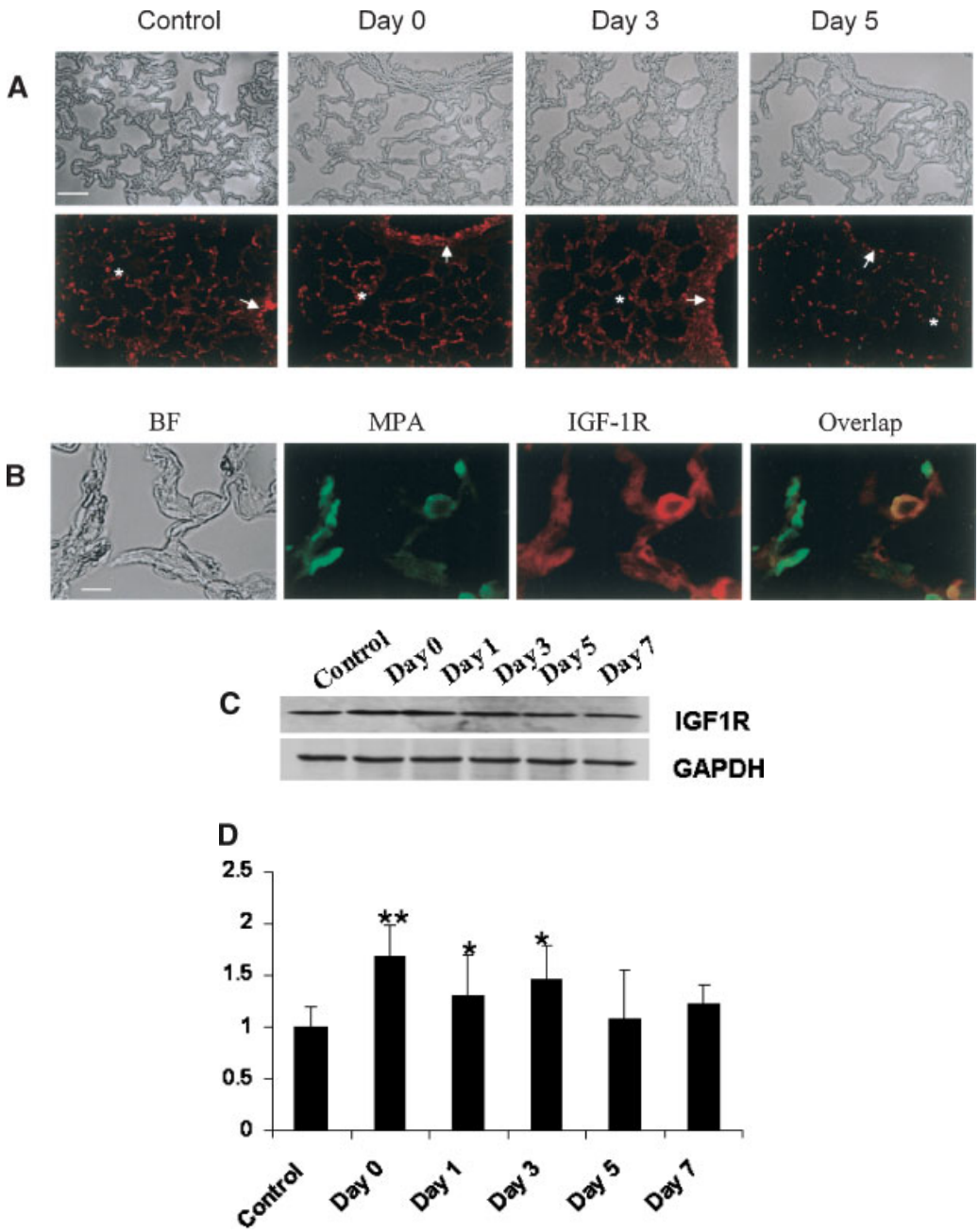

Fig. 5. IGF-1R protein localization and expression in the lung. **A**: Lung tissue were sectioned for immunohisochemistry from air-exposed rats (control), 48 h hyperoxia-exposed (day 0) rats, and rats that were exposed to hyperoxia for 48 h and allow to recover for 3 and 5 days (day 3 and 5). The tissue sections were stained with anti-IGF-1Rβ antibodies. Asterisks illustrate the staining of IGF-1R in alveolar type II cells and arrows the staining in airway epithelium. **Upper panels** are bright fields and **lower panels** immunofluorescence. **B**: Co-localization of IGF-1Rβ IGF-1R with the type II cell marker, MPA. The normal lung tissue was dually labeled with anti-IGF-1Rβ and FITC-MPA. BF, bright field; overlap, overlap images from IGF-1Rβ and MPA. Scale bar, 20 μm. **C**, **D**: Quantitation of IGF-1R protein levels in hyperoxia-injured and recovering lungs. Rats were exposed to air (control) or hyperoxia (>95% O_2) for 48 h (day 0) and allowed to recover for 1–7 days (day 1, 3, 5, and 7). IGF-1R protein levels were determined by Western blot. The blots were probed with GAPDH for loading control. A representative of Western blots for IGF-1R is shown in **panel C**. IGF1R protein levels were qunatitated by densitometry and normalized to GADPH (**panel D**). Data were expressed as a percentage of control (air-exposed lungs) and are presented as mean ± SE. n = 5 independent animal groups. $^{*}P < 0.05$ versus control and $^{**}P < 0.01$ versus control.

with or without anti-IGF-1R, anti-IGF-I, or anti-IGF-II antibodies for 1–5 days. In the absence of the antibodies, the morphological analysis clearly showed the trans-differentiation of type II cells into type I-like cells, which started on day 2, and by day 5 most of the cells acquired the flat and large shape, indicative of type I cells (Fig. 6A). Double-labeling with the type I cell marker, purinergic receptor P2X7 [Chen et al., 2004b], and the type II cell marker, LB-180 [Zen et al., 1998], showed a decrease in LB-180 staining and an increase in P2X7 staining as a function of culture time (Fig. 6A). The addition of IGF-1R antibodies resulted in the retention of the cuboidal shape and LB-180 staining of type II cells, but no staining of P2X7. This was further supported by the observation that the increase of T1 α (another type I cell marker) mRNA and protein levels were partially prevented when the cells were cultured in the presence of anti-IGF-1R (Fig. 6B,C). Inclusion of anti-IGF-I, but not anti-IGF-II antibodies during the culture also prevented the increase of T1 α protein level (Fig. 6C) as well as the morphological change (data not shown).

During the trans-differentiation, the mRNA expression of endogenous IGF-I was slightly elevated on day 1 and a significant increase was noted only on day 2 (Fig. 7A). The expression of IGF-I was decreased to an undetectable level by day 5. In contrast, IGF-II increased from day 2 culture and remained high until day 5 (Fig. 7B).

Finally, we examined the effects of blocking IGF signaling on type II cell proliferation. Type II cells isolated from the 48 h hyperoxia-exposed lungs showed an increase in cell number compared to the cells isolated from normal lungs when cultured for 48 h on plastic dishes (Fig. 8). Furthermore, when the cells from the hyperoxia-exposed lungs were cultured in the presence of anti-IGF-I or anti-IGF-1R antibodies there was a significant decrease in cell number compared to the cells cultured without antibodies. However, anti-IGF-II antibodies had no effects.

DISCUSSION

Our previous studies have demonstrated that exposure to hyperoxia causes a wide spectrum of pathophysiological changes in adult rat lungs [Narasaraju et al., 2003]. Tissue repair occurs when these injured animals return to normoxic conditions. The severity of injury influences the mode of tissue repair, leading to either normal repair in which the regeneration of normal alveolar architecture occurs or abnormal remodeling, which results in tissue fibrosis [Adamson and Bowden, 1974a; O'Brodovich and Mellins, 1985; Adamson et al., 1988]. Previously, several studies have demonstrated an induction of several components in the IGF signaling pathway during hyperoxia-mediated lung injury. The present study utilized a model of lung injury and repair to examine the expression of IGF system components, including IGF-I, II, IGF-1R, 2R, IGFBP-2, 3, 5, and IRS-1 in tissue repair. The salient finding of our study is the involvement of IGF signaling pathway in alveolar epithelial cell proliferation and differentiation during repair after hyperoxia-mediated lung injury. Blocking with antibodies against IGF-I and IGF-1R in vitro demonstrated that IGF-I signaling via IGF-1R is required to promote type II cells proliferate and trans-differentiate into type I cells.

An animal model of lung injury and normal remodeling was used by exposing adult rats to >95% oxygen for 48 h and allowing them to recover in normal air. Histopathological analy-

Fig. 6. Effect of anti-IGF-I and anti-IGF1R antibodies on the trans-differentiation of alveolar type II cells. **A**: Detection of phenotypic change by Double-labeling using type I and type II cell markers. Type II cells isolated from the 48 h hyperoxia (>95% O_2)-exposed rat lungs were cultured on plastic dishes for 1 day (**a**, **d**, **g**, **j**, **m**, and **p**), 3 days (**b**, **e**, **h**, **k**, **n**, and **q**), and 5 days (**c**, **f**, **i**, **l**, **o**, and **r**) in the absence (a–i) or presence (j–r) of 2 μg/ml anti-IGF-1Rβ antibodies. The cells were stained with anti-LB-180 (type II cell marker) (e–f, m–o) and anti-purinergic receptor P2X7 (type I cell marker) (g–l, p–r). The bright fields are shown in a–c and j–l. Scale bar: 20 μm. **B**: mRNA levels of a type I cell marker, T1 α. Type II cells isolated from the 48 h hyperoxia (>95% O_2)-exposed rat lungs were cultured in DEM/F12 medium for 0 day (D0), 1 day (D1), 2 days (D2), 3 days (D3), or 5 days (D5) or in DEM/F12 medium plus 2 μg/ml anti-IGF-1Rβ antibodies for 1 day (D1-anti-IGF1R), 2 days (D2-anti-IGF1R), or 5 days (D5-anti-IGF1R). The mRNA levels were determined by real time PCR. Data was expressed as fold changes over day 0 (D0) after being normalized to 18S rRNA. $^{*}P < 0.05$ versus day 0, $^{**}P < 0.05$ versus day 5, n = 6 (three cell preparations and each assay performed in duplicate). **C**: Western blot for T1 α. Type II cells isolated from the 48 h hyperoxia (>95% O_2)-exposed rat lungs were cultured in DEM/F12 medium (control) or in the presence of anti-IGF I (2 μg/ml), anti-IGF II (2 μg/ml), or anti-IGF 1R (2 μg/ml) for 1–3 days. T1 α protein expressions were determined by Western blot. The blots were also probed with anti-glyceraldehyde-3-phosphate dehydrogenase (GAPDH) antibodies for the loading control. [Color figure can be viewed in the online issue, which is available at www.interscience.wiley.com.]

sis showed the damage of alveolar epithelial lining and type II cell hyperplasia after 48 h of hyperoxia exposure. After 7 days of recovery in ambient air, the alveolar structure was regained without any symptoms of inflammation or fibroblast proliferation. Type II cell number increased after 48 h hyperoxia exposure and remained high until day 3 of recovery. Furthermore, the reduction in type I cell number occurred due to injury, but increased on day 1 of recovery, indicating that cell differentiation begins early in the recovery

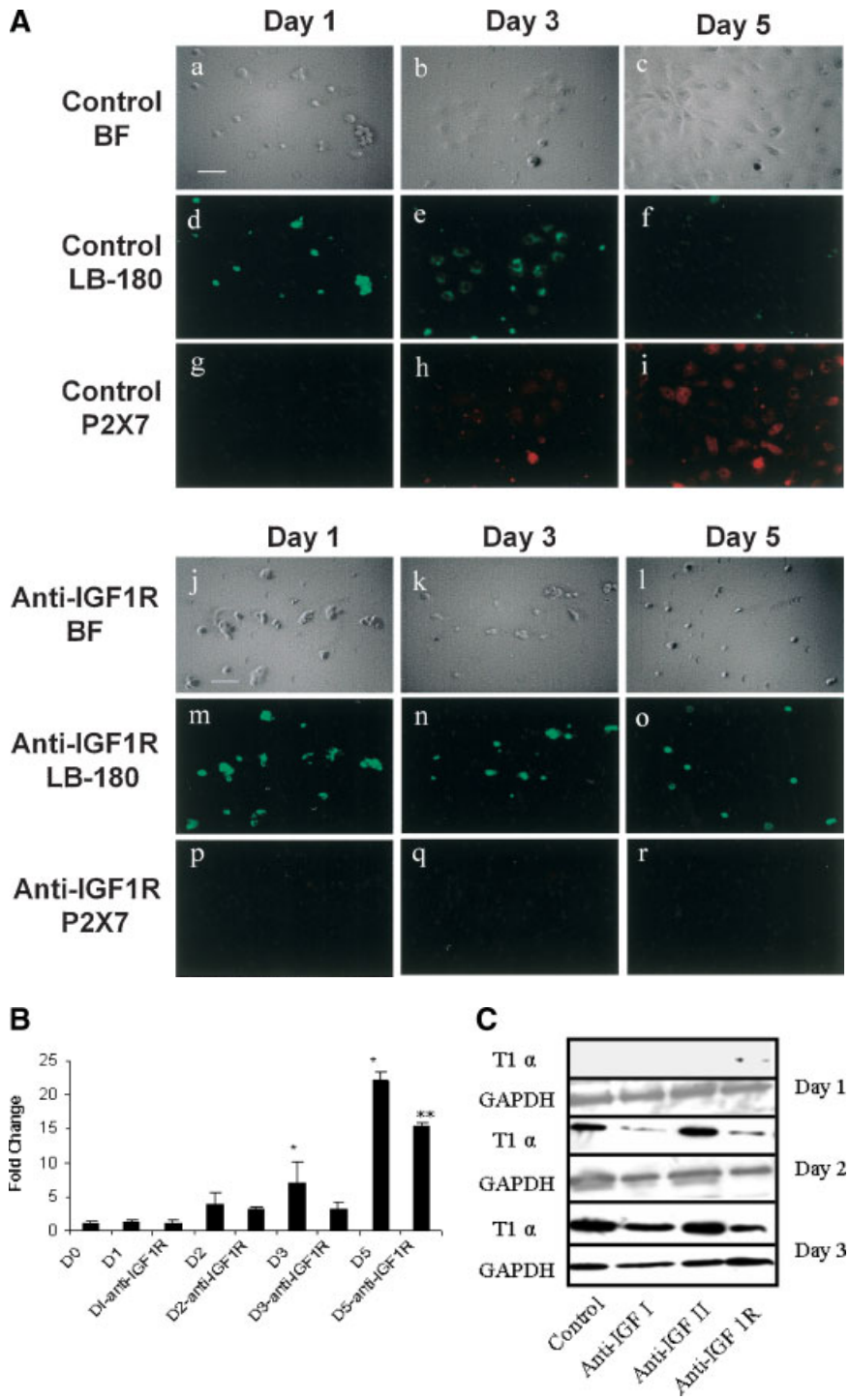

Fig. 6.

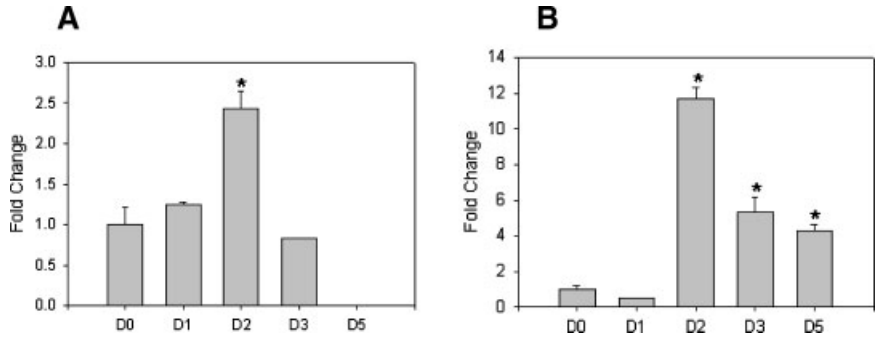

Fig. 7. mRNA expression of IGF-1 and IGF-II in cultured alveolar type II cells. Type II cells were isolated from the 48 h hyperoxia-exposed lungs and cultured on plastic dishes for 0–5 days (D0, D1, D2, D3, and D5). At the end of culture, total RNAs were extracted and the mRNA expression was determined by real-time PCR. Data were expressed as fold changes over D0 after being normalized with 18S rRNA. **Panel A**: IGF-I; **panel B**: IGF-II. $^*P < 0.05$ versus D0, n = 6 (three cell preparations and each assay performed in duplicates).

phase. These results support the widely accepted concept that type II cells proliferate and differentiate into type I cells during tissue repair.

IGFs and their receptors and binding proteins are essential for lung development [Wallen and Han, 1994; Maitre et al., 1995]. Both IGF-I and IGF-II expressions in the lung increased after 48 h exposure to hyperoxia, but remained similar to the control animals during the recovery. Although the mRNA expression of IGF-I and IGF-II were not altered during the recovery, immunostaining showed that protein levels remain high until day 3 of recovery. Two possibilities may exist in explaining these results: (i) IGF-I and IGF-II proteins translation or stability increase during the recovery; or (ii) the increased IGF-I may originate from an extra-pulmonary source such as the liver. Previous studies have shown that mice carrying null mutation of either IGF-I or IGF-1R, die after birth due to respiratory failure and growth deficiency [Liu et al., 1993]. A long-term oxygen exposure increases the expression of IGF-I in mesenchymal cells, leading to fibroblast proliferation [Han et al., 1996]. In another study, the increase in IGF-I was associated with proliferation and migration of fibroblasts [Chetty et al., 1999]. However, in both models, there was very little expression of IGF-I and IGF-II observed in alveolar type II cells. Our present study showed that IGF-I was more abundant in alveolar type II cells and airway epithelium, and only minimum staining was observed in mesenchymal cells. These contradictory results may be due to the exposure time and thus, the severity of injury, which may influence the proliferation in different cell systems.

IGF-1R is a common receptor for both IGF-I and IGF-II. It is a heterotetrameric protein consisting of 2 α-subunits and 2 β-subunits. The binding of IGFs to the α-subunit causes the phosphorylation of the β-subunit and subsequent phosphorylation the down stream substrates such as IRS-1, ultimately leading to cell proliferation through the activation of transcription factors [Adams et al., 2000; LeRoith and Roberts, 2003]. Although the mRNA expression of IGF-1R increased only at day 0, protein levels were elevated until day 3 of recovery, as demonstrated by Western blot and immunohistochemistry. The abundant expression of IGF-1R protein in alveolar type II cells suggests that IGFs may regulate the type II cell proliferation and differentiation observed in this study. Previous studies found IGF-1R expression in alveolar epithelial cells only after 14 days, but not 6 days exposure to 85% oxygen, suggesting that the concentration of oxygen may also influence the gene regulation of IGF system components in the lung.

Since we found the expression of IGF-I and IGF-1R in alveolar type II cells during the injury and tissue repair, we envisage that IGF-I and its receptor may have a key role in the regulation of alveolar epithelial cell proliferation and differentiation. Cell proliferation was increased in the type II cells isolated from hyperoxia-exposed lungs compared to those from normal lungs, suggesting that the hyperoxic type II cells have more potential to proliferate than the normal type II cells. This is consistent with a rise of IGF-I and IGF-IR mRNA and protein in hyperoxic type II cells. Furthermore, anti-IGF-I or anti-IGF-1R antibodies inhibit type II cell proliferation.

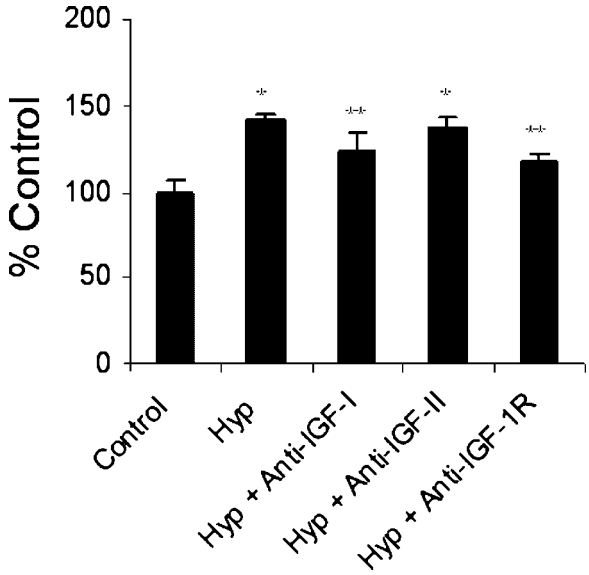

Fig. 8. Effect of anti-IGF-I and -II, and anti-IGF1R antibodies on type II cell proliferation. Type II cells were isolated from the 48 h hyperoxia-exposed lungs and cultured for 48 h in the absence (Hyp) or presence of anti-IGF-I (Hyp + Anti-IGF I), anti-IGF-II (Hyp + Anti-IGF II), or anti-IGF-1R (Hyp + Anti-IGF1R) antibodies (2 μg/ml each). The control was the cells isolated from air-exposed rats. Cell proliferation assay was carried out in a 96-well plate. The data represent mean ± SE. $*P < 0.05$ versus control, $**P < 0.05$ versus Hyp, n = 12 (three cell preparations and each assay performed in four replications).

To examine role of IGF-I in trans-differentiation of type II cells to type I cells, we carried out an in vitro culture study with alveolar type II cells isolated from 48 h hyperoxia-exposed lungs. It is well accepted that the type II cells cultured in vitro plastic dishes trans-differentiate into type I-like cells. When the hyperoxic type II cells were cultured on plastic dishes, the gradual change in morphology from round and cubiodal to large and flat shape was observed, indicating that these type II cells undergo the trans-differentiation into type I-like cells. This was further supported by the increased expression of the type I cell markers, P2X7 and T1 α, the decrease of the type II cell marker, LB-180 during the culture. IGF-I mRNA was also increased during the initial days of type II cell culture. The blocking of IGF-I and IGF-1R, but not IGF-II decreased the expression of P2X7 and T1 α. The cytoplasmic extensions formed during the trans-differentiation of type II cells into type I-like cells was also inhibited by the addition of anti-IGF-1Rβ antibodies, giving direct evidence for the role of IGF-I system in the differentiation of alveolar epithelial type II cells.

In summary, mild hyperoxia exposure causes type I cell injury and type II cell hyperplasia. We speculate that the injury triggers the IGF signaling pathway by enhancing the expressions of IGF-I and IGF-1R in type II cells which proliferate and differentiate into type I cells, thus regenerate normal alveolar epithelium.

ACKNOWLEDGMENTS

The authors thank Dr. Antoinette Wetterwald (University of Berne, Switzerland) and Dr. Mary C. Williams (Boston University) for T1 α (E11) antibodies, Dr. Marcia D. Howard for reading the article, and Candice Marsh for secretary assistance. The authors are also thankful to Shane Miller and Roland Myers (Penn State College of Medicine) for their assistance in histology work. ZC and NJ were supported by predoctoral fellowships from AHA Heartland affiliate 0315260Z and 0315256Z.

REFERENCES

Adams TE, Epa VC, Garrett TP, Ward CW. 2000. Structure and function of the type 1 insulin-like growth factor receptor. Cell Mol Life Sci 57:1050–1093.

Adamson IY, Bowden DH. 1974a. The type 2 cell as progenitor of alveolar epithelial regeneration. A cytodynamic study in mice after exposure to oxygen. Lab Invest 30:35–42.

Adamson IY, Bowden DH. 1974b. The type 2 cell as progenitor of alveolar epithelial regeneration. A cytodynamic study in mice after exposure to oxygen. Lab Invest 30:35–42.

Adamson IY, Young L, Bowden DH. 1988. Relationship of alveolar epithelial injury and repair to the induction of pulmonary fibrosis. Am J Pathol 130:377–383.

Barazzone C, Belin D, Piguet PF, Vassalli JD, Sappino AP. 1996. Plasminogen activator inhibitor-1 in acute hyperoxic mouse lung injury. J Clin Invest 98:2666–2673.

Bhatt AJ, Pryhuber GS, Huyck H, Watkins RH, Metlay LA, Maniscalco WM. 2001. Disrupted pulmonary vasculature and decreased vascular endothelial growth factor, Flt-1, and TIE-2 in human infants dying with bronchopulmonary dysplasia. Am J Respir Crit Care Med 164:1971–1980.

Cazals V, Nabeyrat E, Corroyer S, de Keyzer Y, Clement A. 1999. Role for NF-kappa B in mediating the effects of hyperoxia on IGF-binding protein 2 promoter activity in lung alveolar epithelial cells. Biochim Biophys Acta 1448:349–362.

Chen JW, Chen Z, Narasaraju T, Jin N, Liu L. 2004a. Isolation of highly pure alveolar epithelial type I and type II cells from rat lungs. Lab Invest 84:727–735.

Chen Z, Jin N, Narasaraju T, Chen J, McFarland LR, Scott M, Liu L. 2004b. Identification of two novel markers for

alveolar epithelial type I and II cells. Biochem Biophys Res Commun 319:774–780.

Chetty A, Nielsen HC. 2002. Regulation of cell proliferation by insulin-like growth factor 1 in hyperoxia-exposed neonatal rat lung. Mol Genet Metab 75:265–275.

Chetty A, Faber S, Nielsen HC. 1999. Epithelial–mesenchymal interaction and insulin-like growth factors in hyperoxic lung injury. Exp Lung Res 25:701–718.

Cohick WS, Clemmons DR. 1993. The insulin-like growth factors. Annu Rev Physiol 55:131–153.

Crapo JD, Barry BE, Foscue HA, Shelburne J. 1980. Structural and biochemical changes in rat lungs occurring during exposures to lethal and adaptive doses of oxygen. Am Rev Respir Dis 122:123–143.

Delhanty PJ, Hill DJ, Shimasaki S, Han VK. 1993. Insulin-like growth factor binding protein-4, -5 and -6 mRNAs in the human fetus: localization to sites of growth and differentiation? Growth Regul 3:8–11.

Han VK, Lauder JM, D'Ercole AJ. 1988. Rat astroglial somatomedin/insulin-like growth factor binding proteins: Characterization and evidence of biologic function. J Neurosci 8:3135–3143.

Han RN, Han VK, Buch S, Freeman BA, Post M, Tanswell AK. 1996. Insulin-like growth factor-I and type I insulin-like growth factor receptor in 85% O_2-exposed rat lung. Am J Physiol 271:L139–L149.

Harris JB, Chang LY, Crapo JD. 1991. Rat lung alveolar type I epithelial cell injury and response to hyperoxia. Am J Respir Cell Mol Biol 4:115–125.

Jones JI, Clemmons DR. 1995. Insulin-like growth factors and their binding proteins: Biological actions. Endocr Rev 16:3–34.

Jones JI, Gockerman A, Busby WH, Jr., Wright G, Clemmons DR. 1993. Insulin-like growth factor binding protein 1 stimulates cell migration and binds to the alpha 5 beta 1 integrin by means of its Arg-Gly-Asp sequence. Proc Natl Acad Sci USA 90:10553–10557.

Kitterman JA, Chapin CJ, Vanderbilt JN, Porta NF, Scavo LM, Dobbs LG, Ertsey R, Goerke J. 2002. Effects of oligohydramnios on lung growth and maturation in the fetal rat. Am J Physiol Lung Cell Mol Physiol 282:L431–L439.

Kueng W, Silber E, Eppenberger U. 1989. Quantification of cells cultured on 96-well plates. Anal Biochem 182: 16–19.

LeRoith D, Roberts CT, Jr. 2003. The insulin-like growth factor system and cancer. Cancer Lett 195:127–137.

Liu JP, Baker J, Perkins AS, Robertson EJ, Efstratiadis A. 1993. Mice carrying null mutations of the genes encoding insulin-like growth factor I (Igf-1) and type 1 IGF receptor (Igf1r). Cell 75:59–72.

Maitre B, Clement A, Williams MC, Brody JS. 1995. Expression of insulin-like growth factor receptors 1 and 2 in the developing lung and their relation to epithelial cell differentiation. Am J Respir Cell Mol Biol 13:262–270.

Narasaraju TA, Jin N, Narendranath CR, Chen Z, Gou D, Liu L. 2003. Protein nitration in rat lungs during hyperoxia exposure: A possible role of myeloperoxidase. Am J Physiol Lung Cell Mol Physiol 285:L1037–L1045.

Nici L, Medina M, Frackelton AR. 1996. The epidermal growth factor receptor network in type 2 pneumocytes exposed to hyperoxia in vitro. Am J Physiol 270:L242–L250.

O'Brodovich HM, Mellins RB. 1985. Bronchopulmonary dysplasia. Unresolved neonatal acute lung injury. Am Rev Respir Dis 132:694–709.

Stewart CE, Rotwein P. 1996. Growth, differentiation, and survival: Multiple physiological functions for insulin-like growth factors. Physiol Rev 76:1005–1026.

Veness-Meehan KA, Moats-Staats BM, Price WA, Stiles AD. 1997. Re-emergence of a fetal pattern of insulin-like growth factor expression during hyperoxic rat lung injury. Am J Respir Cell Mol Biol 16:538–548.

Wallen LD, Han VK. 1994. Spatial and temporal distribution of insulin-like growth factors I and II during development of rat lung. Am J Physiol 267:L531–L542.

Yam J, Frank L, Roberts RJ. 1978. Oxygen toxicity: Comparison of lung biochemical responses in neonatal and adult rats. Pediatr Res 12:115–119.

Zen K, Notarfrancesco K, Oorschot V, Slot JW, Fisher AB, Shuman H. 1998. Generation and characterization of monoclonal antibodies to alveolar type II cell lamellar body membrane. Am J Physiol 275:L172–L183.